1997

H2S adsorption on chromium, chromia, and gold/chromia surfaces: Photoemission studies

J A. Rodriguez

S Chaturvedi

U Diebold

M Kuhn

J van Ek

See next page for additional authors

Recommended Citation

J. Chem. Phys. 107, 9146 (1997)

H_2S adsorption on chromium, chromia, and gold/chromia surfaces: Photoemission studies

J. A. Rodriguez and S. Chaturvedi
Department of Chemistry, Brookhaven National Laboratory, Upton, New York 11973

M. Kuhn, J. van Ek, and U. Diebold
Department of Physics, Tulane University, New Orleans, Louisiana 70118

P. S. Robbert, H. Geisler, and C. A. Ventrice, Jr.
Department of Physics, University of New Orleans, New Orleans, Louisiana 70148

(Received 10 June 1997; accepted 26 August 1997)

The reaction of H_2S with chromium, chromia, and Au/chromia films grown on a Pt(111) crystal has been investigated using synchrotron-based high-resolution photoemission spectroscopy. At 300 K, H_2S completely decomposes on polycrystalline chromium producing a chemisorbed layer of S that attenuates the Cr $3d$ valence features. No evidence was found for the formation of CrS_x species. The dissociation of H_2S on Cr_3O_4 and Cr_2O_3 films at room temperature produces a decrease of 0.3–0.8 eV in the work function of the surface and significant binding-energy shifts (0.2–0.6 eV) in the Cr $3p$ core levels and Cr $3d$ features in the valence region. The rate of dissociation of H_2S increases following the sequence: $Cr_2O_3 < Cr_3O_4 < Cr$. For chromium, the density of states near the Fermi level is large, and these states offer a better match in energy for electron acceptor or donor interactions with the frontier orbitals of H_2S than the valence and conduction bands of the chromium oxides. This leads to a large dissociation probability for H_2S on the metal, and a low dissociation probability for the molecule on the oxides. In the case of Cr_3O_4 and Cr_2O_3, there is a correlation between the size of the band gap in the oxide and its reactivity toward H_2S. The uptake of sulfur by the oxides significantly increases when they are ''promoted'' with gold. The Au/Cr_2O_3 surfaces exhibit a unique electronic structure in the valence region and a larger ability to dissociate H_2S than polycrystalline Au or pure Cr_2O_3. The results of *ab initio* SCF calculations for the adsorption of H_2S on $AuCr_4O_6$ and $AuCr_{10}O_{15}$ clusters show a shift of electrons from the gold toward the oxide unit that enhances the strength of the $Au(6s) \leftrightarrow H_2S(5a_1,2b_1)$ bonding interactions and facilitates the decomposition of the molecule. © *1997 American Institute of Physics.* [S0021-9606(97)01945-4]

I. INTRODUCTION

One of the most severe poisonings encountered in catalytic systems is that induced by sulfur on metal/oxide catalysts.[1] In industrial applications the life time of a supported metal catalyst can be reduced to only a few months or weeks in the presence of ppm quantities of sulfur contaminants in petroleum-derived feedstreams.[1] Millions of dollars are lost every year in the chemical and oil industries due to the effects of sulfur poisoning on the performance of metal/oxide catalysts.[1] In spite of the importance of this problem, a detailed knowledge of the factors that control the mechanisms of sulfur poisoning at a microscopic level does not exist.[1] This type of fundamental knowledge can provide novel ideas for improving the sulfur tolerance of industrial catalysts.

Model systems generated by vapor depositing a metal onto ultrathin oxide films have recently emerged as a promising way to investigate the behavior of supported metal catalysts.[2–8] These model systems feature many of the advantages of metal single crystals (i.e., they can be characterized by means of surface sensitive techniques where either electrons or ions are used) while still addressing important issues such as the effects of particle size and metal-support interactions.[5] Exploiting the utility of this approach, we have started a research program aimed at gaining a better understanding of the effects of sulfur on the physical and chemical properties of metal/oxide surfaces.[9–11] In our previous works we have examined the interaction of sulfur with metal/alumina surfaces.[9,10] In such systems the large band gap in the oxide support ($\sim$9 eV, Ref. 12) leads to very weak sulfur $\leftrightarrow$alumina interactions, and sulfur attacks mainly the supported metal.[9,10] In the present work, we study the adsorption of H_2S on clean and gold ''promoted'' oxides of chromium. For these systems the band gap of the oxide is relatively small ($<$5 eV, Ref. 13) and the supported metal, in principle, has a low affinity toward sulfur.[14]

Chromia is an active catalyst for the hydrogenation and isomerization of alkenes, methanol synthesis, and the reduction of nitric oxides.[15] Pure and uniform bulk samples of single-crystal chromium oxides are very difficult to prepare. Chromium oxide films offer a convenient and useful route for studying the surface chemistry of chromia.[6,16] Recently, the feasibility of growing well-ordered chromium oxide films on Pt(111) with thicknesses ranging from less than a monolayer to more than eight monolayers has been shown.[17] The films were grown by Cr vapor deposition in an O_2 background pressure. The growth mode, structure, and the ther-

 0021-9606/97/107(21)/9146/11/$10.00

mal stability of the resulting overlayers were studied using a combination of ion-scattering spectroscopy, x-ray photoelectron spectroscopy (XPS), low-energy electron diffraction (LEED), and scanning tunneling microscopy (STM).[17] For the first two monolayers, a well-ordered $p(2\times2)$ structure is observed. The overlayer symmetry and core-level XPS data are consistent with the epitaxial growth of Cr_3O_4.[17] At higher coverages, a $(\sqrt{3}\times\sqrt{3})R30°$ structure appears due to the formation of the Cr_2O_3 phase.[17] Photoemission measurements and first principles density functional calculations indicate that in the $p(2\times2)$ phase the ''metallic character'' (i.e., reduced oxidation state of Cr and electron emissions at the Fermi level) is much more pronounced than in the Cr_2O_3 phase.[13] The theoretical calculations predict the Cr_3O_4 phase to be metallic (as its iron analog Fe_3O_4).[13] Bulk Cr_2O_3, on the other hand, is known to be an insulating material. Our results show a correlation between the ''metallic character'' and the reactivity of the chromium oxide films toward H_2S. In addition, Au clusters (or 3D particles) supported on Cr_2O_3 exhibit a much larger reactivity toward H_2S than those seen either for the pure oxide or bulk Au.

II. EXPERIMENT

The experiments were carried out at the U4A beam line of the National Synchrotron Light Source (NSLS) at Brookhaven National Laboratory. This beam line is equipped with a 6 m toroidal grating monochromator and an ultrahigh vacuum chamber (base pressure $<2\times10^{-10}$ Torr) fitted with a hemispherical electron energy analyzer and instrumentation for LEED. The valence spectra were taken with photon energies of 155, 75, and 50 eV, while photon energies of 195 (S $2p$ region) and 155 eV (Cr $3p$ and Au $4f$ regions) were used to acquire the core-level spectra. The binding-energy scale in the photoemission spectra was calibrated with respect to the position of the Fermi edge at a given photon energy. There was no problem with sample charging during these studies. The overall instrumental resolution in the photoemission experiments was 0.25–0.30 eV. Work function measurements were made by biasing the sample negatively (-14 V) and recording the photoemission onset and Fermi edge using a photon energy of 75 eV to excite the electrons.

The Pt(111) substrate, on which the chromia films were grown, was cleaned following standard procedures reported in the literature.[14,17] The Pt crystal was mounted on a manipulator capable of liquid nitrogen cooling to 100 K and heating to 2000 K. Heating was achieved by electron bombardment from behind the sample. A W-5% Re/W-26%Re thermocouple was spot welded to the edge of the Pt(111) sample for temperature measurements.

Films of chromium oxide were grown on Pt(111) following a methodology described in a previous work.[17] Chromium atoms (generated by heating a W wire wrapped around a high-purity pellet of Cr) were dosed on the platinum substrate at 500–600 K in a background O_2 pressure of 2×10^{-6} Torr to form the chromium oxide films. This was followed by annealing at 600–700 K for 5 min. The coverage (or thickness) of the chromium oxide films was determined using LEED and the ratio of the Pt $4f$ and Cr $3p$ peaks in the photoemission spectra.[17] Gold was vapor deposited on the CrO_x/Pt(111) systems at 300 K. The evaporation of gold was achieved by resistively heating a W filament wrapped by an ultrapure wire of Au. The atomic flux from the metal doser was calibrated according to the methodology described in our previous studies for Au/Pt(111).[14b] The CrO_x and Au/CrO_x surfaces were exposed to H_2S at room temperature. After doing this, the coverage of sulfur was determined by measuring the area under the S $2p$ peaks, which was scaled to absolute units by comparing to the corresponding area for 0.33 ML of atomic sulfur on Pt(111).[14]

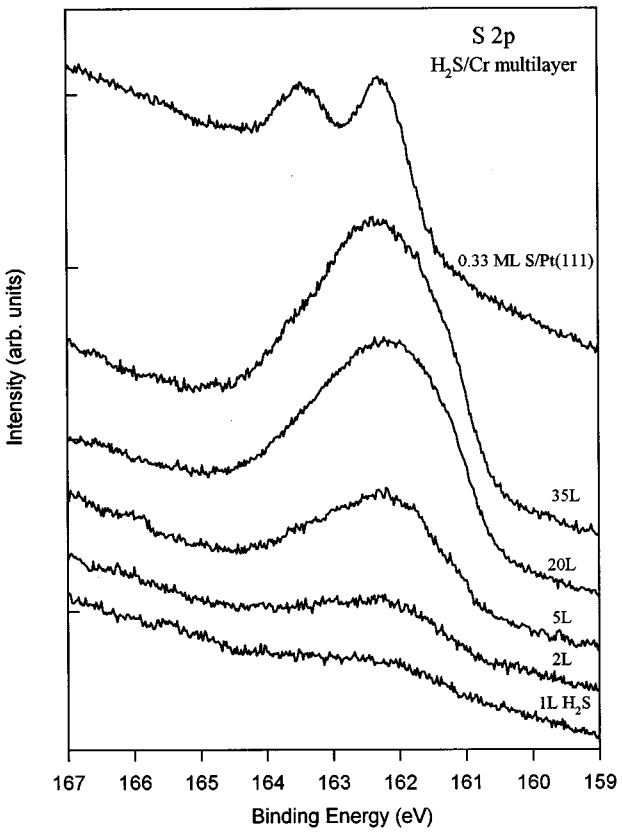

FIG. 1. Sulfur $2p$ spectra for the adsorption of H_2S on a chromium multilayer ($\theta_{Cr}>10$ ML) at 300 K. The doses of H_2S are reported in Langmuir (1 L$=10^{-6}$ Torr/•s). At the top of the figure is shown the S $2p$ spectrum for 0.33 ML of S on Pt(111). The spectra were acquired using a photon energy of 195 eV.

III. RESULTS

A. H_2S adsorption on chromium

Figure 1 shows S $2p$ spectra acquired after dosing H_2S on a polycrystalline chromium film (>10 ML) at 300 K. For comparison we also include the corresponding spectrum for 0.33 ML of S on Pt(111). This spectrum shows a well-defined doublet for the S $2p_{1/2}$ and $2p_{3/2}$ features. Separation of these features is not observed in the case of the H_2S/Cr systems, probably due to the roughness of the surface (i.e., more than one adsorption site) or the existence of chemically

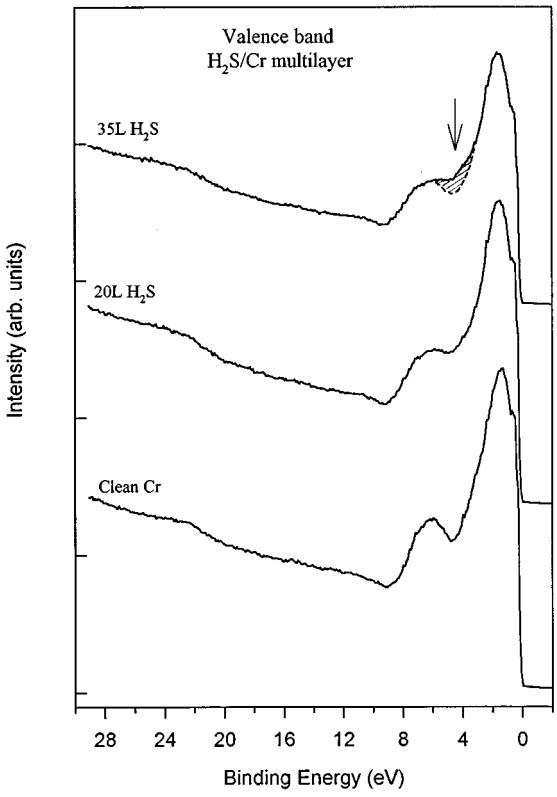

FIG. 2. Valence spectra acquired after exposing a Cr film ($\theta_{Cr}>10$ ML) to 20 and 35 L of H_2S at 300 K (photon energy=75 eV). In the top spectrum, the hatched area indicates additional intensity not seen for clean Cr.

different sulfur atoms. The H_2S/Cr systems exhibit S $2p$ peak positions (162.0–162.5 eV) that are very close in energy to those found after the dissociation of S_2 on Cr (Ref. 18) and smaller than those reported for H_2S or HS chemisorbed on metals (163.5–165 eV, Refs. 19–21). This indicates that H_2S fully decomposes into sulfur and hydrogen on the chromium surface. An identical result has been observed after dosing H_2S to Cu,[21] Ni,[20] Mo,[19,22] Pt[23] and Ru[24] surfaces at room temperature.

The valence spectra for the H_2S/Cr systems in Fig. 2 show an absence of the photoemission peaks associated with chemisorbed H_2S and HS in the region between 8 and 14 eV,[24] and extra intensity in the region around 4 eV that is not seen in the spectrum for clean Cr (see arrow and hatched area). Following previous works for S/Pt(111),[25] S/W(001),[26] and S/Ru(001),[27] we assign the new ''features'' at $\sim$4 eV to emission of electrons from the $3p$ orbitals of atomic sulfur. In Fig. 1, the uptake of sulfur by the Cr surface is close to 0.8 ML after a dose of 35 L of H_2S. At this point the dissociative adsorption of H_2S induced a decrease of $\sim$0.3 eV in the work function of the system. The dissociation of H_2S did not lead to significant changes in the binding energy of the Cr $3p$ features ($\Delta BE \leqslant 0.1$ eV). This behavior is in contrast with that observed for S_2/Cr systems ($\theta_s>1$ ML),[18] where the formation of CrS_x produces shifts of 0.4–0.6 eV in the binding energy of the Cr $2p$ core levels. Thus it is likely that the S atoms created by the decomposition of H_2S remain in a chemisorbed state on top of the Cr surface.

B. H_2S adsorption on Cr_3O_4

In this section we describe the results for the reaction of H_2S with chromium oxide films that were 1–2 ML thick. These films exhibited a $p(2\times2)$ LEED pattern as seen in previous studies.[17] It has been proposed that the $p(2\times2)$ pattern comes from a Cr_3O_4 overlayer oriented with its (111) surface parallel to the Pt(111) surface.[17] Because Cr_3O_4 and Pt have the same underlaying fcc Bravais lattice, the growth of Cr_3O_4(111) is favored by the metal substrate.[17] In this configuration, close-packed hexagonal planes of oxygen are separated by cation layers in which Cr^{2+} and Cr^{3+} are present. Indeed, the results of XPS show the presence of Cr^{2+} and Cr^{3+} species in the ultrathin oxide films.[17] The exact structural geometry of these films is unknown, but photoemission data show that they have the band structure and ''metallic character'' expected for Cr_3O_4.[13] In this work, for simplicity, we will refer to these chromium oxide films as ''1 ML'' and ''2 ML Cr_3O_4.''

The top panel of Fig. 3 shows a typical S $2p$ spectrum for the adsorption of H_2S on a 2 ML thick Cr_3O_4 film. A well-defined doublet of peaks is observed for the S $2p_{1/2}$ and $2p_{3/2}$ features. These features appear at binding energies that are very close to those seen after the dissociation of S_2 on ZnO,[11] and lower than those reported for H_2S and SH chemisorbed on metals and sulfides (163.5–165 eV).[19–21] The last difference indicates that H_2S undergoes complete dissociation upon adsorption on Cr_3O_4 at 300 K. This conclusion is also supported by the valence spectra for the H_2S/Cr_3O_4 systems, which showed an absence of the peaks typically associated with adsorbed H_2S and HS in the region between 8 and 14 eV. The Cr_3O_4 films displayed a reactivity toward H_2S that was somewhat smaller than that found for polycrystalline Cr. For example, after exposing a 2 ML Cr_3O_4 film to 55 L of H_2S the coverage of sulfur on the surface was close to 0.5 ML, whereas a dose of 35 L of H_2S produced a sulfur coverage of $\sim$0.8 ML on metallic Cr.

The dissociative adsorption of H_2S induced a decrease of 0.2–0.4 eV in the work function of the Cr_3O_4/Pt(111) systems. At the same time, there were positive shifts of 0.4–0.6 eV in the binding energy of the Cr $3p$ features for the Cr_3O_4 overlayers (see bottom panel of Fig. 3). Figure 4 displays valence spectra acquired before and after dosing 55 L of H_2S to a 2 ML Cr_3O_4 film. The peaks at 2 and 4 eV are primarily from to the oxide overlayer, while the features between 1 and 0 eV are mostly from the Pt substrate.[13] The dissociation of H_2S leads to a broadening and a binding-energy shift of $\sim+0.5$ eV in the Cr_3O_4 peak that appears around 2 eV. From these results one can conclude that H_2S is able to induce significant changes in the electronic properties of Cr_3O_4.

C. H_2S adsorption on Cr_2O_3

Cr_2O_3 is the most common bulk oxide of chromium. In our previous work for CrO_x/Pt(111),[17] it was found that be-

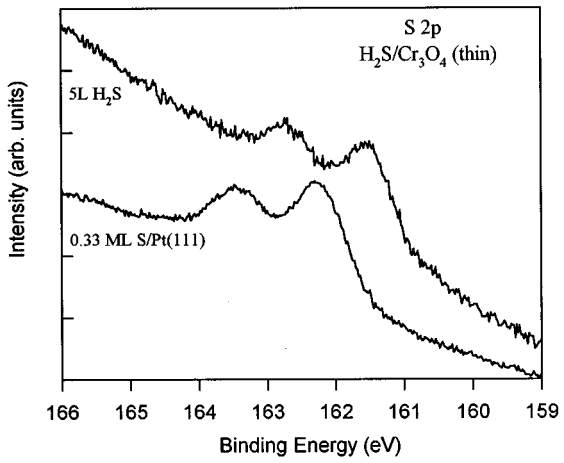

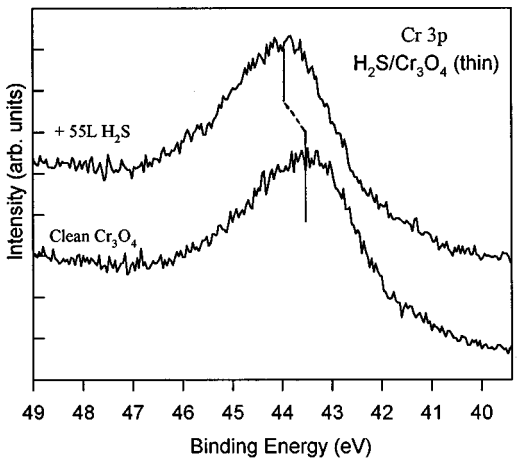

FIG. 3. Top: S $2p$ spectra for 0.33 ML of S on Pt(111) and a 2 ML Cr_3O_4 film exposed to 5 L of H_2S at 300 K. The electrons were excited using a photon energy of 195 eV. Bottom: Cr $3p$ spectra for a clean and H_2S exposed 2 ML Cr_3O_4 film. Photon energy: 155 eV.

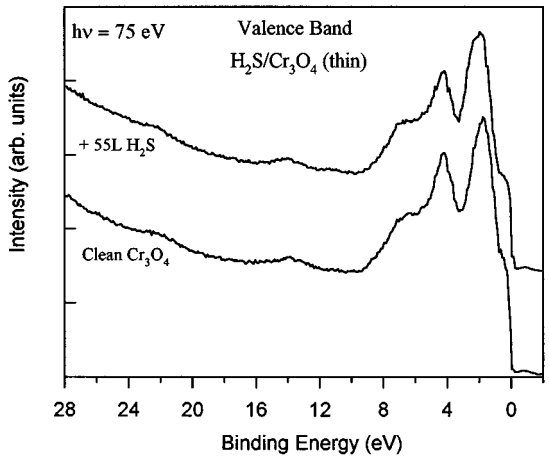

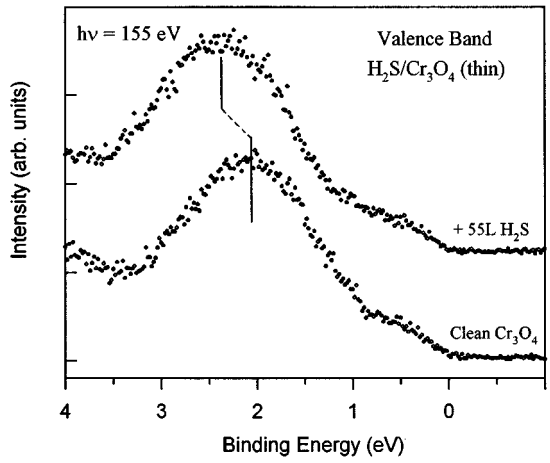

FIG. 4. Effects of H_2S on the valence band of a 2 ML Cr_3O_4 film. Hydrogen disulfide was dosed at 300 K and the spectra were taken using photon energies of 75 (top) and 155 eV (bottom).

yond a thickness of two monolayers Cr_2O_3 appears and grows epitaxially on top of Cr_3O_4, which wets the substrate. In this section, we will deal with the adsorption of H_2S on a Cr_2O_3 overlayer with a thickness of $\sim$4 ML, and on a relatively thick Cr_2O_3 film (>6 ML). The thick Cr_2O_3 film did not show a well-defined pattern in LEED, whereas the 4 ML Cr_2O_3 film showed a diffuse $(\sqrt{3}\times\sqrt{3})R30\,^\circ$ pattern. This $(\sqrt{3}\times\sqrt{3})R30\,^\circ$ structure can be attributed to a Cr_2O_3 overlayer with its (0001) face parallel to Pt(111).[17] Overall, the Cr_2O_3 systems studied in this work are best described as polycrystalline.

Figure 5 displays the amount of sulfur deposited on the two Cr_2O_3 films after exposing them to various doses of H_2S at 300 K. Among all the systems investigated in our study, the thick Cr_2O_3 film showed the lowest reactivity toward H_2S. For example, a dose of 22 L of H_2S on the thick Cr_2O_3 film at 300 K produced a sulfur coverage of $\sim$0.15 ML, which is much smaller than the sulfur coverages of $\sim$0.4 and 0.7 ML found after dosing 20 L of H_2S on 2 ML Cr_3O_4 and Cr (respectively). For the conditions in Fig. 5, results of photoemission for the S $2p$ and valence regions indicate that there was a complete decomposition of H_2S on the Cr_2O_3 surfaces. The S $2p$ spectra showed binding energies that were close to those observed in Fig. 3 for atomic sulfur on Cr_3O_4, but on the Cr_2O_3 systems the spectra were broader and there was not a clear separation between the $2p_{1/2}$ and $2p_{3/2}$ features (a typical result is shown in the top panel of Fig. 6). This is consistent with the fact that the Cr_2O_3 surfaces were less ordered (i.e., more rough, with different types of adsorption sites) than the 2 ML Cr_3O_4 surface, as indicated by LEED.

In the valence spectra for the H_2S/Cr_2O_3 systems, we did not find any peak that indicated the existence of chemisorbed H_2S or SH when the H_2S exposures were smaller than 50 L. After a H_2S dose of 100 L to the thick Cr_2O_3 film, we observed a new peak at $\sim$9 eV in the valence region (bottom panel of Fig. 6). This peak suggests the presence of SH species on the surface of the oxide,[24] and disappeared upon annealing the sample to 450 K. For the interaction of H_2S with metals,[19–24] it is well known that adsorbed SH is stable only when the very reactive sites of the surface are blocked (or ''poisoned'') by sulfur atoms. It appears that a

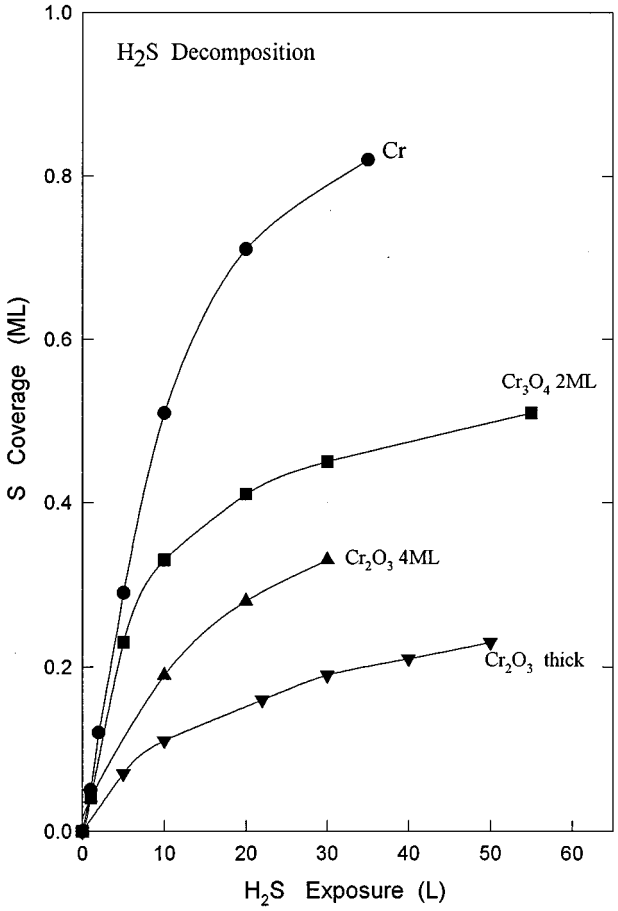

FIG. 5. Amount of sulfur adsorbed on Cr (●), 2 ML Cr_3O_4 (■), 4 ML Cr_2O_3 (▲), and thick Cr_2O_3 (▼) as a function of H_2S exposure. The adsorption experiments were carried out at 300 K.

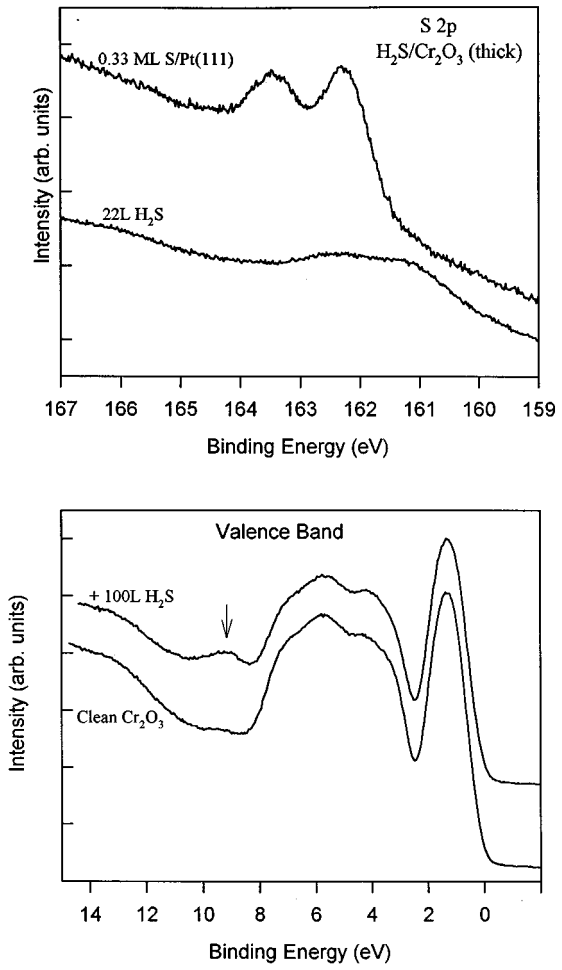

FIG. 6. S $2p$ (top panel, photon energy 195 eV) and valence spectra (bottom panel, photon energy 50 eV) taking after exposing a thick Cr_2O_3 film (>6 ML) to H_2S at 300 K. At the top of the figure, for comparison, we also include the S $2p$ spectrum for 0.33 ML of S on Pt(111).

similar phenomenon occurs on the surface of the Cr_2O_3 oxide.

The interaction with H_2S led to substantial changes in the electronic properties of the Cr_2O_3 films. Upon the deposition of S (0.1–0.2 ML), there was a substantial decrease (0.5–0.8 eV) in the work function of these systems. This was accompanied by positive binding-energy shifts (0.3–0.4 eV) in the Cr $3p$ core levels.

D. H_2S adsorption on Au/Cr_3O_4 and Au/Cr_2O_3 surfaces

In a set of experiments we examined the interaction of H_2S with a polycrystalline gold film (>10 ML) at 300 K. For H_2S doses as large as 40 L, we did not find any evidence for the adsorption or dissociation of the molecule on the gold surface. After a dose of 150 L of H_2S there was a trace of sulfur (<0.05 ML) on the gold, and a dose of 400 L of H_2S produced only a small sulfur coverage (~0.08 ML). These findings are consistent with previous studies for the $H_2S/Au(111)$[28] and $H_2S/Au(110)$ systems,[29,30] where H_2S is adsorbed molecularly (heat of adsorption =7–10 kcal/mol) and desorbs at temperatures below 250 K. H_2S does not dissociate on Au(111) or Au(110).[28,30] Minor decomposition of the molecule has been observed after producing defect sites on the Au surfaces by sputtering,[30] or after irradiating an adsorbed layer of H_2S with electrons.[28–30]

Figure 7 displays Au $4f$ and S $2p$ spectra recorded after depositing 1.5 ML of Au on a 2 ML Cr_3O_4 film that had been exposed to 5 L of H_2S ($\theta_s \sim 0.25$ ML). The intensity observed for the Au $4f$ peaks is much smaller than those observed for 1 ML of Au on polycrystalline Cr or Pt(111) where Au wets the metal substrate.[14b] At the same time, the deposition of Au did not produce any significant reduction in the Cr $3p$ signal of the oxide film. This indicates that Au is forming three-dimensional (3D) clusters or islands on the H_2S/Cr_3O_4 system,[14] and is also consistent with a migration of S from the oxide to on top of gold (see below) that attenuates the Au $4f$ signal. Previous studies have shown that Au does not wet well the surfaces of oxides[7,31] or metal surfaces precovered with sulfur.[14,32] The deposition of Au on the H_2S/Cr_3O_4 system leads to almost no change in the intensity of the S $2p$ features, and they shift to lower binding energy to a position near that for sulfur atoms adsorbed on

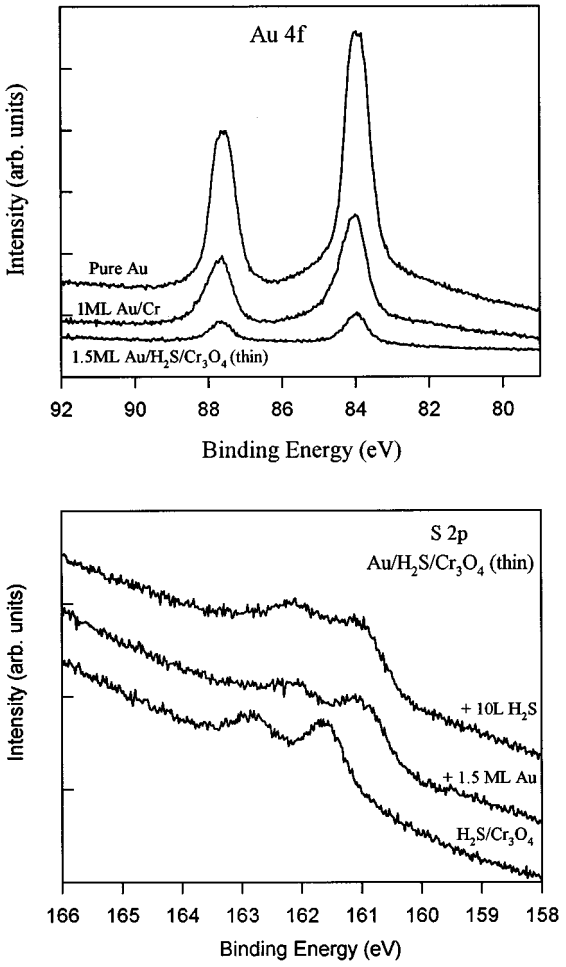

FIG. 7. Top: Au $4f$ spectra for pure Au, 1 ML of Au on metallic Cr, and 1.5 ML of Au on a 2 ML Cr_3O_4 film precovered with $\sim$0.3 ML of sulfur (photon energy $=$155 eV). Bottom: S $2p$ spectra for a 2 ML Cr_3O_4 film exposed to H_2S ($\theta_S \sim 0.25$ ML), then ''promoted'' with 1.5 ML of Au, and finally exposed to 10 L of H_2S ($T=300$ K; photon energy $=$195 eV).

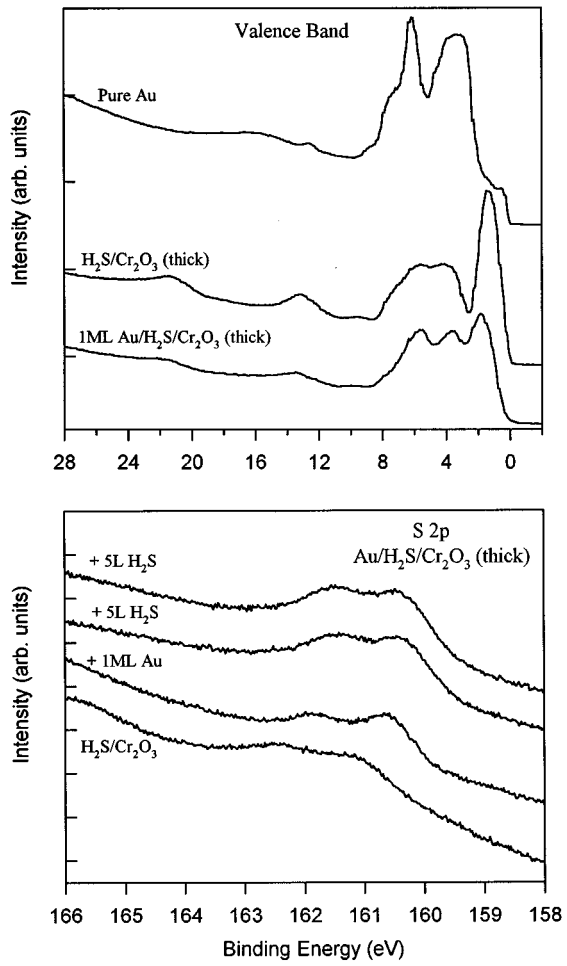

FIG. 8. Top: Valence band spectra for pure Au, and a thick Cr_2O_3 film ($>$6 ML) exposed to H_2S and then ''promoted'' with 1 ML of Au (photon energy$=$75 eV). Bottom: S $2p$ spectra for the thick Cr_2O_3 film exposed to H_2S ($\theta_S \sim 0.2$ ML), then ''promoted'' with 1 ML of Au, and finally exposed to two successive doses of 5 L of H_2S ($T=300$ K; photon energy$=$195 eV).

gold.[14,30,33] This behavior suggests that a large fraction of the adsorbed sulfur is migrating from the oxide substrate to on top of the Au clusters. A similar phenomenon has been seen after depositing Au on S/Mo(100) surfaces[32] and is, in part, a consequence of the low surface-free energy of sulfur.[34] In Fig. 7, after exposing the $Au/H_2S/Cr_3O_4$ system to an additional 10 L of H_2S, one sees a significant increase in the coverage of sulfur. The final sulfur coverage is approximately 0.4 ML. To obtain such a coverage on a clean Cr_3O_4 film, one needs a H_2S dose of 20 L. Thus it appears that the Au/Cr_3O_4 system is somewhat more reactive toward H_2S than clean Cr_3O_4 or bulk Au.

For the interaction of Au with the H_2S/Cr_3O_4 and H_2S/Cr_2O_3 systems, the qualitative trends were identical. In all the cases examined the Au $4f$ signal was small (3D clustering of Au), the S $2p$ features were not attenuated and they shifted toward lower binding energy on Au deposition (possible migration of S from the oxide substrate of the admetal), and the Au ''promoted'' surfaces were able to decompose H_2S at 300 K in a relatively easy way. This is best illustrated by the results for the interaction of Au with a thick Cr_2O_3 film ($>$6 ML). The top panel in Fig. 8 shows a valence spectrum taken after depositing a monolayer of Au on a thick Cr_2O_3 film that had been previously exposed to 40 L of H_2S ($\theta_s \sim 0.2$ ML). This spectrum shows an electronic structure that is substantially different from those of pure Au, and the Cr_2O_3 (Ref. 13) and H_2S/Cr_2O_3 surfaces. This change in the valence levels of the system correlates with an increase in its reactivity toward H_2S. The bottom panel of Fig. 8 shows how the S $2p$ spectrum of the H_2S/Cr_2O_3 system changes after depositing Au and dosing H_2S. The deposition of Au produces a negative shift of $\sim$0.6 eV in the S $2p$ features without inducing a significant reduction in their intensity. Subsequent dosing of 10 L of H_2S leads to an increase of $\sim$0.25 ML in the amount of sulfur present in the system. To generate this coverage on a thick Cr_2O_3 film, one needs H_2S exposures in excess of 40 L, and more than 400 L on the polycrystalline Au. Thus the interaction between the Au clusters and the chromia support produces a system that has

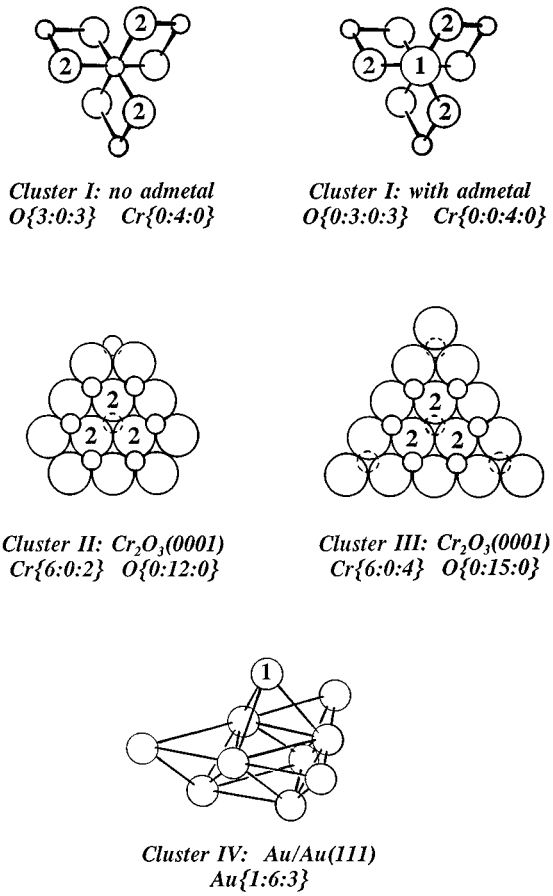

FIG. 9. Different views (or projections) of the clusters used to model the adsorption of H_2S on Au/Cr_2O_3 (I–III) and Au (IV). Clusters I, II, and III have three layers of pure Cr or O atoms. The notation $\{a:b:c\}$ specifies how many Cr (small circles) or O atoms (large circles) are in each layer. A gold atom was deposited on the center of the three-fold hollow site formed by the oxygen atoms labeled ''2'' in clusters I, II, and III. In the *ab initio* SCF calculations, the H_2S molecule was bonded to this Au atom or to the Au atom labeled ''1'' in cluster IV.

a unique electronic structure (see above) and a large ability to adsorb and dissociate H_2S.

An analysis of the S $2p$ positions for the spectra at the bottom of Fig. 8 indicates that most of the sulfur present on the Au/Cr_2O_3 surfaces is bonded to the admetal. Therefore, it is reasonable to conclude that the active sites for the dissociation of H_2S involve Au atoms. The large reactivity of these Au atoms may come from the fact that they form small metal clusters or may be a result of electronic perturbations induced by the oxide support. To explore the second possibility, we decided to investigate the effects of chromia on the $H_2S \leftrightarrow Au$ interactions at a molecular orbital level using *ab initio* self-consistent-field (SCF) calculations[35] and the clusters shown in Fig. 9. Cluster I ($Au+Cr_4O_6$) is a model for an Au atom supported on a defect site of chromia in which the oxygen atoms have a relatively low coordination number. It probably maximizes admetal$\leftrightarrow$oxide interactions. Clusters II ($Au+Cr_8O_{12}$) and III ($Au+Cr_{10}O_{15}$) were used to study the deposition of Au on a $Cr_2O_3(0001)$ surface. This surface

TABLE I. Theoretical results for the adsorption of H_2S on Au and Au/Cr_2O_3 clusters.

System	Adsorp. Energy [a] (kcal/mol)	Au–S (Å)	S–H (Å)	Molec. plane tilting
$AuAu_9$	3.4	2.69	1.33	11°
$AuCr_4O_6$	14.6	2.64	1.34	16°
$AuCr_8O_{12}$	11.8	2.61	1.34	18°
$AuCr_{10}O_{15}$	10.3	2.61	1.34	18°

[a]Following the standard convention, positive values denote an exothermic adsorption process.

produces a $(\sqrt{3}\times\sqrt{3})R30°$ LEED pattern[17] similar to that observed for some of the Cr_2O_3 films employed in our work. Cluster IV ($Au+Au_9$) represents an Au atom in contact with a Au(111)-like particle.

For clusters I–III, the Cr–O bond distances were all set equal to 2.0 Å(an average of the distances of 1.97 and 2.02 Å found in Cr_2O_3, Ref. 36), the O–Cr–O angles were 90°, and the $Au-O_2$ distances were optimized at the *ab initio* SCF level obtaining values of 2.22–2.26 Å. In cluster IV, the Au–Au bond lengths and angles were set equal to those observed in bulk gold.[37] Figure 10[10] displays the bonding configuration for H_2S when the molecule was adsorbed on a supported gold atom. Spectroscopic evidence[38–41] shows that hydrogen sulfide is adsorbed on metals making bonds through the sulfur, with its molecular plane either parallel or tilted with respect to the surface normal. For the free H_2S molecule, the calculated S–H bond distances (1.33 Å) and H–S–H bond angle (94 °) agree very well with the reported experimental values (1.33 Å, 92 °).[42] The adsorption of H_2S did not produce significant changes in the geometry of the molecule. Table I shows the optimal adsorption geometries found in our calculations for H_2S on $AuCr_4O_6$, $AuCr_8O_{12}$, and $AuAu_9$. (For the adsorption of H_2S on $AuCr_{10}O_{15}$, a system with a relatively large number of atoms, we used the bonding geometry obtained for H_2S on $AuCr_8O_{12}$ without further optimization.) The values predicted for the Au–S bond lengths (2.61–2.69 Å) are similar to those observed in x-ray diffraction studies for inorganic complexes that contain Au–S bonds.[43] According to the SCF calculations H_2S should be adsorbed with its molecular plane slightly tilted (11–18 °) with respect to the surface normal, but the difference in bonding energy between perpendicular and tilted adsorption was small ($\leqslant$1.8 kcal/mol) in all the cases.

For the Cr_4O_6, Cr_8O_{12}, and $Cr_{10}O_{15}$ clusters, we found that the occupied $\{O\ 2p+Cr\ 3d,4s\}$ states appeared at energies between -6 and -16 eV, with the empty $\{Cr\ 3d,4s+O\ 2p\}$ states located at energies above -1 eV (for a typical result, see Fig. 11). The ''band'' gap observed in the SCF calculations (6.1–6.8 eV) was somewhat bigger than that seen in bulk Cr_2O_3 (4.8 eV, Ref. 17). Nevertheless, the ''band'' structure predicted by the SCF calculations for the oxide clusters was in general agreement with that observed for bulk Cr_2O_3 in first-principles density functional calculations.[13] In Fig. 10, we show a rough picture for the frontier orbitals of H_2S. The calculated energies for the $5a_1$ and $2b_1$ orbitals are in excellent agreement with the corre-

sponding ionization potentials (13.20 and 10.31 eV, respectively).[38] In principle, the bonding mechanism of H_2S to an oxide or metal can involve donation of charge from the ''S lone pairs'' ($5a_1$ and $2b_1$ orbitals) into the surface and back donation of electrons from the surface into the H_2S ($3b_2$) orbital.[40,41] By comparing the results in Figs. 10 and 11, we can see that the match in energy for an interaction between the molecule ''S lone pairs'' and the empty bands of Cr_2O_3, or the occupied bands of Cr_2O_3 and the LUMO of H_2S, is very poor. On the other hand, a gold atom with a half occupied $6s$ orbital at -7.7 eV provides a relatively good match for an electron-acceptor interaction with the $5a_1$ and $2b_1$ orbitals of H_2S. We found that a gold atom supported on the clusters of Fig. 9 exhibited positive charges:[45] $0.32e$ in $AuCr_4O_6$, $0.24e$ in $AuCr_8O_{12}$, $0.27e$ in $Cr_{10}O_{15}$, and $0.08e$ in $AuAu_9$. In the $AuCr_4O_6$ and $AuCr_{10}O_{15}$ systems, there was a significant shift of electrons from the admetal toward the oxide support that increased the stability of the half empty Au($6s$) orbital by 1.7–2.3 eV and, therefore, facilitated Au($6s$)$\leftrightarrow H_2S(5a_1,2b_1)$ bonding interactions.

In Table I are listed the calculated adsorption energies for H_2S on clusters I–IV. Our SCF calculations did not include effects of electron correlation. Thus it is likely that the values listed in Table I underestimate the bonding energy of the molecule on the clusters.[46,47] This fact explains why the calculated bonding energy for H_2S on the $AuAu_9$ cluster (3.4 kcal) is smaller than the adsorption energy of H_2S on Au(111) and Au(110) surfaces (7–10 kcal/mol).[28–30,41] In Table I, one can see a clear increase in the adsorption energy of H_2S when Au is supported on the chromium-oxide clusters. These results suggest that the large reactivity seen in the experiments of Fig. 8 for Au/Cr_2O_3 can be a consequence of electronic perturbations induced by the oxide support on gold.

IV. DISCUSSION

A. H_2S adsorption on Cr, Cr_3O_4, and Cr_2O_3 systems

The experiments described above indicate that Cr_2O_3 is much less reactive toward H_2S than metallic chromium. The reactivity seen on polycrystalline Cr is comparable to that found for the dissociation of H_2S on other early transition metals (W, Ref. 26 and Mo, Refs. 19,22). For chromium, there is a large density of states immediately above or below the Fermi level, and these states offer a better match in energy for electron acceptor or electron donor interactions with the orbitals of H_2S than the valence and conduction bands of Cr_2O_3 (see Fig. 11). This leads to a large dissociation probability for H_2S on the metal, and a low dissociation probability for the molecule on the oxide.

The results for the interaction of H_2S with the different oxide films show an increase in reactivity that follows the sequence: thick $Cr_2O_3 < 4$ ML $Cr_2O_3 < 2$ ML Cr_3O_4 (see Fig. 5). This trend cannot be attributed to a rise in the number of defect sites on the oxide surface, since according to LEED the degree of order in the oxide systems also increased following the sequence: thick Cr_2O_3 (no LEED pattern) <4 ML Cr_2O_3 [diffuse $(\sqrt{3}\times\sqrt{3})R30°$ pattern] <2 ML Cr_3O_4 [clear $p(2\times2)$ pattern]. The Cr_2O_3 surfaces are more rough than the 2 ML Cr_3O_4 surface, and this leads to S $2p$ spectra that are more broad and ill defined (compare Figs. 3 and 6). Thus among the oxide films, the Cr_3O_4 system exhibits the largest reactivity toward H_2S and have the lowest number of defect sites on the surface. First-principles density functional calculations and photoemission experiments show very large differences in the band structures of Cr_3O_4 and Cr_2O_3.[13] The theoretical studies indicate that, in essence, there is no band gap around the Fermi level of Cr_3O_4.[13] This oxide exhibits a much larger ''metallic character'' than Cr_2O_3, with a high density of states immediately above and below the Fermi level.[13] The match in energy between the bands of Cr_3O_4 and the frontier orbitals of H_2S is better than for the H_2S/Cr_2O_3 system, and this difference seems to have a direct impact on the reactivity of the oxides toward H_2S.

Studies for the S_2/Al_2O_3 (Refs. 9,10) and S_2/ZnO (Ref. 11) systems also indicate that there is a correlation between the size of the band gap in an oxide and its reactivity toward S-containing molecules. For example, after exposing films of Al_2O_3 (bulk band gap $\sim$9 eV, Ref. 12) to large amounts of S_2 (enough to produce AlS_x multilayers on Al), sulfur coverages smaller than 0.1 ML are observed.[10] However, similar S_2 doses on ZnO (bulk band gap $\sim$3.4 eV, Ref. 48) produce sulfur coverages close to 0.7 ML.[11] When comparing our results for H_2S/Cr_2O_3 with those previously reported for S_2/Al_2O_3,[10] one has to keep in mind that S_2 is a much more reactive molecule than H_2S. Nevertheless, it is easier to generate a S coverage close to 0.1 ML in the H_2S/Cr_2O_3 system than in S_2/Al_2O_3 due to the smaller band gap in Cr_2O_3 ($\sim$4.8 eV, Ref. 17).

Thiols (RSH) are common impurities present in oil-derived feedstreams used in the chemical industry.[49] These species have frontier orbitals similar to those of H_2S,[50,51] and their decomposition reactions ($RSH_{gas}\rightarrow RS_a + H_a$; $RSH_{gas}\rightarrow S_a + RH_{gas}$) are more exothermic than those of H_2S.[40,50] Our results suggest that oxides with a small band gap (SnO_2, ZnO, TiO_2, Cr_2O_3, etc.) should be more susceptible to S poisoning by thiol decomposition than oxides in which the band gap is big (Al_2O_3, MgO, CaO, etc.).

B. H_2S adsorption on Au/chromia surfaces

In previous works, we have examined the interaction of sulfur with metal/alumina surfaces (AM/Al_2O_3, AM=Cu, Zn, or Ag).[9,10] In such systems the large band gap in the oxide support leads to very weak sulfur$\leftrightarrow$alumina interactions, and sulfur attacks mainly the supported metal.[9,10] The adsorption of sulfur induces drastic changes in the electronic properties of the admetal, and frequently one sees the formation of admetal sulfides (AMS_x) that decompose at temperatures above 700 K (which are higher than the temperatures typically used in most catalytic processes).[9,10] In the Au/chromia systems one is dealing with an oxide support that has a relatively small band gap,[13] which should enhance S $\leftrightarrow$oxide interactions with respect to $S/AM/Al_2O_3$, and Au is

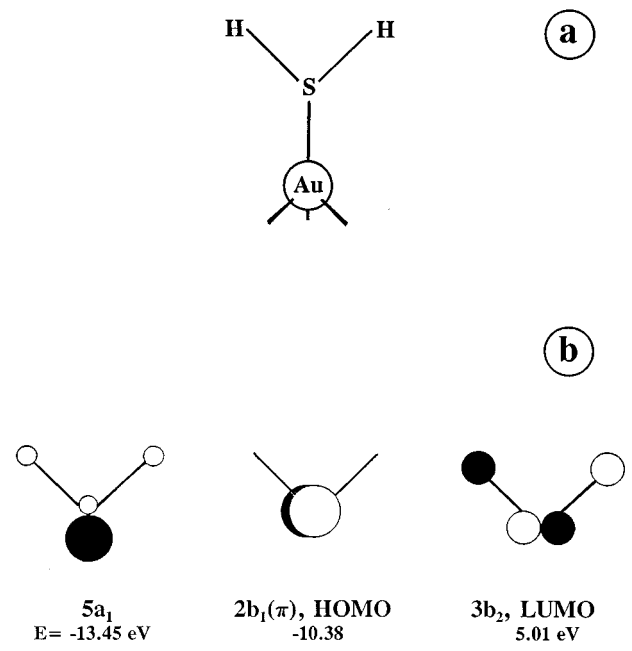

FIG. 10. (a) Bonding configuration for H_2S on an Au atom supported on chromia or Au(111). (b) Rough picture for the frontier orbitals of H_2S. The displayed MO energies come from our *ab initio* SCF calculations and are very close to the experimental ionization potentials (Ref. 38).

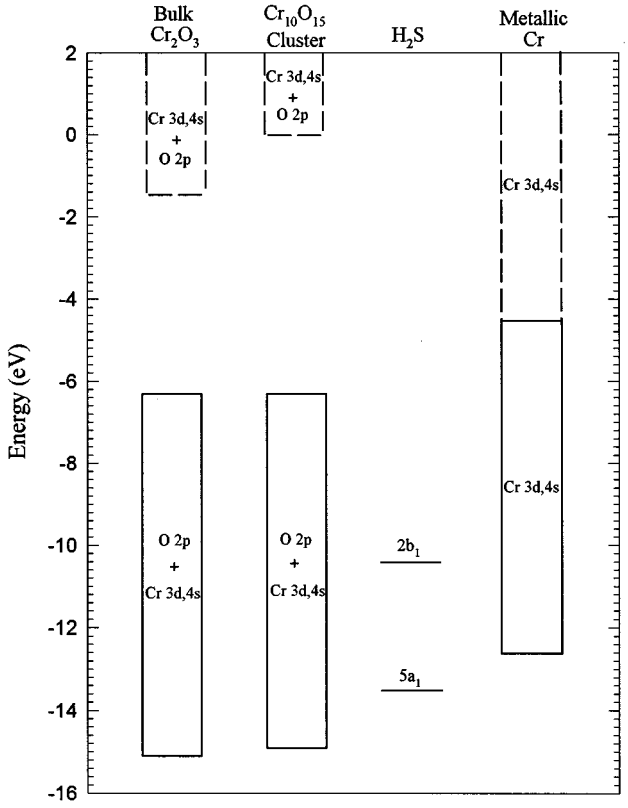

FIG. 11. Energy positions for the bands of bulk Cr_2O_3, the $Cr_{10}O_{15}$ cluster and metallic Cr. The empty and occupied states are indicated by dashed and solid lines, respectively. The position for the valence bands of Cr was estimated using work function measurements (Ref. 44) and photoemission data (Fig. 2). To estimate the position for the valence and conduction bands of bulk Cr_2O_3, we used photoemission data (Ref. 13) (aligning the top of the occupied $\{O\ 2p+Cr\ 3d,4s\}$ band with the corresponding energy calculated for the $Cr_{10}O_{15}$ cluster) and the reported experimental value for the band gap (Ref. 17). For comparison, we also include the calculated energies for the $5a_1$ and $2b_1$ orbitals of H_2S. The energies are reported with respect to the vacuum level.

probably the metal with the lowest affinity toward sulfur in the Periodic Table,[14] which should favor S↔oxide interactions instead of S↔admetal interactions. In spite of these facts, the S↔admetal interactions are stronger than the S ↔oxide interactions in the H_2S/Au/chromia systems. For the deposition of Au on S/chromia surfaces, the results of XPS show shifts in the S $2p$ features and a lack of attenuation in the S signal that suggest a migration of adsorbed S from the oxide substrate to the admetal. The behavior of the Au/S/Cr_3O_4 system is particularly interesting because, even when the oxide support has metallic properties,[13] sulfur prefers to bond to the admetal.

The Au/Cr_2O_3 surfaces exhibit a larger ability to dissociate H_2S than polycrystalline Au or pure Cr_2O_3. This enhancement in reactivity is probably a consequence of the unique electronic structure that the Au/Cr_2O_3 surfaces display in their valence spectra (Fig. 8). In principle, three phenomena may be responsible for the large reactivity of Au ''promoted'' Cr_2O_3: (1) electronic interactions between the admetal and oxide can produce oxide sites that are more chemically active than those in Cr_2O_3; (2) the supported Au clusters can have an intrinsic activity bigger than that of bulk Au; and (3) the oxide support can electronically perturb Au raising its reactivity. The first possibility can be discarded because most of the sulfur adsorbed on the Au/H_2S/Cr_2O_3 systems seems to be bonded to Au and not to the oxide. With respect to the second possibility, it is known that small clusters of noble metals have special structural and electronic properties that can make them very reactive.[7] Finally, the third possibility is substantiated by the *ab initio* SCF calculations in Sec. III D. These calculations show a shift or polarization of electrons from Au toward the Cr_2O_3 substrate that increases the magnitude of the Au$(6s)$↔$H_2S(5a_1,2b_1)$ bonding interactions and facilitates the decomposition of the molecule. In the literature a few systems have been reported in which Au becomes chemically active due to bonding with other metals (Au/Ru(001), Refs. 52–54 and Au/Pd(110), Ref. 55) or with an oxide (Au/TiO_2, Ref. 56).

V. CONCLUSIONS

(1) Polycrystalline Cr is very reactive toward H_2S. At 300 K, the molecule completely decomposes producing a chemisorbed layer of sulfur that substantially attenuates the intensity of the Cr $3d$ band near the Fermi level. No evidence was found for the formation of CrS_x species.

(2) For the adsorption of H_2S on chromium oxides the rate of dissociation of the molecule increases in the following sequence: $Cr_2O_3 < Cr_3O_4 < Cr$. There is a correlation between the ''metallic character'' (i.e., reduced oxidation state

of Cr and large density of states at the Fermi level) and the reactivity of an oxide toward H_2S. At 300 K, the dissociation of H_2S on Cr_3O_4 and Cr_2O_3 surfaces induces a decrease of 0.3–0.8 eV in the work function and significant binding-energy shifts (0.2–0.6 eV) in the Cr $3p$ core levels.

(3) For the Au/S/chromia systems, the Au↔S interactions are stronger than the S↔oxide interactions. The Au/Cr_2O_3 surfaces exhibit a unique electronic structure in the valence region and a larger ability to dissociate H_2S than polycrystalline Au or pure Cr_2O_3. The results of *ab initio* SCF calculations show a shift or polarization of electrons from Au toward the Cr_2O_3 substrate that increases the magnitude of the Au($6s$)↔$H_2S(5a_1,2b_1)$ bonding interactions and facilitates the decomposition of the molecule.

ACKNOWLEDGMENTS

The authors would like to thank H.-S. Tao for his help with the use of the U4A beamline at the NSLS, and J. Hrbek for the loan of a Pt(111) crystal. The NSLS is supported by the Divisions of Materials and Chemical Sciences of the U.S. Department of Energy. The work carried out at BNL was also supported under Contract No. DE-AC02-76CH00016 with the U.S. Department of Energy, Office of Basic Energy Sciences, Chemical Science Division. The work performed at TU was supported by LEQSF(1994-97) RD-A-26, the Petroleum Research Fund, the Center for Photoinduced Processes (NSF-EPSCOR), and DOE-EPSCOR. P.S.R. acknowledges support from the BORSF.

[1] (a) C.H. Bartholomew, P.K. Agrawal, and J.R. Katzer, Adv. Catal. **31**, 135 (1982); (b) P.G. Menon, Chem. Rev. **94**, 1021 (1994); (c) J. Oudar and H. Wise, eds. *Deactivation and Poisoning of Catalysts* (Marcel Dekker, New York, 1991).
[2] J.G. Chen, M.L. Colianni, W.H. Weinberg, and J.T. Yates, Surf. Sci. **279**, 223 (1992), and references therein.
[3] Y. Wu, E. Garfunkel, and T.E. Madey, J. Vac. Sci. Technol. A **14**, 1662 (1996).
[4] H. Cordatos T. Bunluesin, J. Stubenrauch, J.M. Vohs, and R.J. Gorte, J. Phys. Chem. **100**, 785 (1996).
[5] (a) D.W. Goodman, Chem. Rev. **95**, 523 (1995); (b) D.R. Reiner, C. Xu, P.M. Holmblad, and D.W. Goodman, J. Vac. Sci. Technol. A **15**, 1653 (1997).
[6] H.-J. Freund, H. Kuhlenbeck, and V. Staemmler, Rep. Prog. Phys. **59**, 283 (1996).
[7] C.T. Campbell, Surf. Sci. Rep. **27**, 1 (1997).
[8] (a) J.A. Rodriguez, M. Kuhn, and J. Hrbek, J. Phys. Chem. **100**, 18 240 (1996); (b) D.G. van Campen and J. Hrbek, J. Phys. Chem. **99**, 16 389 (1995).
[9] J. A. Rodriguez and M. Kuhn, J. Phys. Chem. B **101**, 3187 (1997).
[10] J.A. Rodriguez, M. Kuhn, and J. Hrbek, Surf. Sci. **380**, 397 (1997).
[11] S. Chaturvedi J.A. Rodriguez, and J. Hrbek, J. Phys. Chem. (submitted).
[12] (a) S. Ciraci and I.P. Batra, Phys. Rev. B **28**, 982 (1983); (b) E.T. Arakawa and M.W. Williams, J. Phys. Chem. Solids **29**, 735 (1968); (c) A. Balzarotti and A. Bianconi, Phys. Status Solidi B **76**, 689 (1976).
[13] P.S. Robbert, H. Geisler, C. A. Ventrice, J. van Ek, M. Kuhn, U. Diebold, S. Chaturvedi, and J. A. Rodriguez (unpublished).
[14] (a) M. Kuhn and J.A. Rodriguez, Chem. Phys. Lett. **231**, 199 (1994); (b) J.A. Rodriguez, M. Kuhn, and J. Hrbek, J. Phys. Chem. **100**, 3799 (1996); **100**, 15 494 (1996).
[15] H.H. Kung, *Transition Metal Oxides: Surface Chemistry and Catalysis*, in *Studies in Surface Science Catalysts*, Vol. 45 (Elsevier, New York, 1989).
[16] C.A. Ventrice, D. Erhrlich, E.L. Garfunkel, B. Dillmann, D. Heskett, and H.-J. Freund, Phys. Rev. B **46**, 12 892 (1992), and references therein.
[17] L. Zhang, M. Kuhn, and U. Diebold, Surf. Sci. **375**, 1 (1997).
[18] unpublished.
[19] S.Y. Li, J.A. Rodriguez, J. Hrbek, H.H. Huang, and G.-Q. Xu, Surf. Sci. **366**, 29 (1996).
[20] D.R. Huntley, Surf. Sci. **240**, 13 (1990), and references therein.
[21] C.T. Campbell and B.E. Koel, Surf. Sci. **183**, 100 (1987).
[22] J.L. Gland, E.B. Kollin, and F. Zaera, Langmuir **4**, 118 (1988).
[23] R.J. Koestner, M. Salmeron, E.B. Kollin, and J.L. Gland, Surf. Sci. **172**, 668 (1986).
[24] (a) G.B. Fisher, Surf. Sci. **87**, 215 (1979); (b) J. Lin, J. A. May, S. Didziulis, and E. I. Solomon, J. Am Chem. Soc. **114**, 4718 (1992).
[25] J.A. Rodriguez, M. Kuhn, and J. Hrbek, Chem. Phys. Lett. **251**, 13 (1996).
[26] D.R. Mullins, P.F. Lyman, and S.H. Overbury, Surf. Sci. **277**, 64 (1992).
[27] J. Hrbek, M. Kuhn, and J.A. Rodriguez, Surf. Sci. **356**, L423 (1996).
[28] A.J. Leavitt and T.P. Beebe, Surf. Sci. **314**, 23 (1994).
[29] D.M. Jaffey and R.J. Madix, Surf. Sci. **258**, 359 (1991).
[30] B. Frühberger, M. Grunze, and D.J. Dwyer, J. Phys. Chem. **98**, 609 (1994).
[31] (a) C. Xu and D.W. Goodman, Chem. Phys. Lett. **263**, 13 (1996); (b) C. Xu, W.S. Oh, G. Liu, D.Y. Kim, and D.W. Goodman, J. Vac. Sci. Technol. A **15**, 1261 (1997); (c) L. Zhang, R. Persaud, T. E. Madey, and F. Cosandey (unpublished).
[32] J.C. Dunphy, C. Chapelier, D.F. Ogletree, and M.B. Salmeron, J. Vac. Sci. Technol. B **12**, 1742 (1994).
[33] After dosing 400 L of H_2S to an Au film at 300 K ($\theta_S \sim 0.08$ ML), the sulfur adatoms showed a S $2p_{3/2}$ binding energy of 160.8 eV.
[34] L.Z. Mezey and J. Giber, Jpn. J. Appl. Phys. **21**, 1569 (1982).
[35] (a) The MO calculations were carried out using the HONDO program (Ref. 35b). The nonempirical effective core potentials (ECP's) of Hay and Wadt (Ref. 35c) were used to describe the inner shells of Cr and Au. The ECP for Au included relativistic effects (Ref. 35c). The $1s$ shell of O was described through the ECP generated by Stevens, Basch, and Krauss (Ref. 35d). For sulfur and hydrogen, we included all their electrons in the calculations. The molecular orbitals were expanded using Gaussian-type orbitals. The atomic orbitals of S and H were expressed in terms of a double-zeta quality basis set augmented with polarization functions (Refs. 9,35b). A basis set obtained through a ($3s2p5d/2s1p2d$) contraction scheme (Ref. 35e) was used to describe the $4s$, $4p$, and $3d$ atomic orbitals of Cr. The $6s$, $6p$, and $5d$ atomic orbitals of Au were expressed in terms of a ($3s3p4d/2s1p2d$) basis set (Ref. 35f). Finally, the valence orbitals of O were treated using the basis set recommended by Stevens-Basch-Krauss (Ref. 35d); (b)M. Dupuis, S. Chin, and A. Marquez, in *Relativistic and Electron Correlation Effects in Molecules and Clusters*, edited by G. L. Malli, NATO ASI Series (Plenum, New York, 1992); (c) P.J. Hay and W.R. Wadt, J. Chem. Phys. **82**, 270 (1985); (d) W.J. Stevens, H. Basch, and M. Krauss, *ibid.* **81**, 6026 (1984); (e) L. Zhang, M. Kuhn, U. Diebold, and J.A. Rodriguez, J. Phys. Chem. B **101**, 4588 (1997); (f) J.A. Rodriguez and M. Kuhn, Surf. Sci. **330**, L657 (1995).
[36] R.W.G. Wyckoff, *Crystal Structures*, 2nd ed. (Wiley, New York, 1964), Vol. 2, pp. 6–7.
[37] C. Kittel, *Introduction to Solid State Physics*, 6th ed. (Wiley, New York, 1986), p. 23.
[38] (a) B. Roos and P. Siegbahn, Theor. Chim. Acta **21**, 368 (1971); (b) K. Siegbahn, C. Nordling, G. Johansson, I. Hedman, P. F. Heden, K. Hamrin, U. Gelius, T. Bergmark, L. O. Werme, R. Manne, and Y. Baer, *ESCA Applied to Free Molecules* (North-Holland, Amsterdam, 1969).
[39] A.G. Baca, M.A. Shultz, and D.A. Shirley, J. Chem. Phys. **81**, 6304 (1984).
[40] J.A. Rodriguez, Surf. Sci. **234**, 421 (1990), and references therein.
[41] H. Sellers, Surf. Sci. **294**, 99 (1993).
[42] T.H. Edwards, N.K. Moncur, and L.E. Snyder, J. Chem. Phys. **46**, 2139 (1967).
[43] G. Wilkinson, R.D. Gillard, and J. McCleverty, eds., *Comprehensive Coordination Chemistry* (Pergamon, New York, 1987), Chaps. 16 and 55.
[44] H.B. Michelson, J. Appl. Phys. **48**, 4729 (1977).
[45] (a) The charges were calculated using a Mulliken population analysis (Ref. 45b). Due to the limitations of this type of analysis (Ref. 45c), they must not be considered in quantitative terms; (b) R.S. Mulliken, J. Chem. Phys. **23**, 1841 (1955); (c) A. Szabo and N. S. Ostlund, *Modern Quantum Chemistry* (McGraw-Hill, New York, 1989).
[46] (a) J.L. Whitten and H. Yang, Surf. Sci. Rep. **24**, 55 (1996); (b) R.A. van Santen and M. Neurock, Catal. Rev. Sci. Eng. **37**, 557 (1995).
[47] H. Sellers, A. Ulman, Y. Shnidman, and J.E. Eilers, J. Am. Chem. Soc. **11**, 9389 (1993).

[48] V.E. Henrich and P.A. Cox, *The Surface Science of Metal Oxides* (Cambridge University Press, Cambridge, 1994), p. 111.
[49] J.G. Speight, *The Chemistry and Technology of Petroleum*, 2nd ed. (Dekker, New York, 1991), pp. 233–238.
[50] J.A. Rodriguez Surf. Sci. **278**, 326 (1992).
[51] R.F. Hout, W.J. Pietro, and W.J. Hehre, *A Pictorial Approach to Molecular Structure and Reactivity* (Wiley, New York, 1984).
[52] B. Sakakini, A.J. Swift, J.C. Vickerman, C. Harendt, and K. Christmann, J. Chem. Soc. Faraday Trans. I **83**, 1975 (1987).
[53] J.A. Rodriguez and J. Hrbek, J. Chem. Phys. **97**, 9427 (1992).
[54] M. Kuhn, A. Bezowski, T.K. Sham, J.A. Rodriguez, and J. Hrbek, Thin Solid Films **283**, 209 (1996).
[55] P.J. Schmitz, H.C. Kang, W.-Y. Leung, and P.A. Thiel, Surf. Sci. **248**, 287 (1991).
[56] (a)M. Haruta, N. Yamada, T. Kobayashi, and S. Iijima, J. Catal. **115**, 301 (1989); (b) S.D. Lin, M. Bollinger, and M.A. Vannice, Catal. Lett. **17**, 245 (1993).